

pubs.acs.org/JACS Communication

Acid-Induced, Oxygen-Atom Defect Formation in Reduced Polyoxovanadate-Alkoxide Clusters

Eric Schreiber, Brittney E. Petel, and Ellen M. Matson*



Cite This: https://dx.doi.org/10.1021/jacs.0c03864



ACCESS

Metrics & More



Supporting Information

ABSTRACT: Here, we present the first example of acid-induced, oxygen-atom abstraction from the surface of a polyoxometalate cluster. Generation of the oxygen-deficient vanadium oxide, $[V_6O_6(OC_2H_5)_{12}]^{1-}$, was confirmed via independent synthesis. Spectroscopic analysis using infrared and electronic absorption spectroscopies affords resolution of the electronic structure of the oxygen-deficient cluster (oxidation state distribution = $[V^{III}V^{IV}_{5}]$). This work has direct implications toward the elucidation of possible mechanisms of acid-assisted vacancy formation in bulk transition metal oxides, in particular electron—proton codoping that has recently been described for vanadium oxide (VO_2) . Ultimately, these molecular models deepen our understanding of proton-dependent redox chemistry of transition metal oxide surfaces.

Inderstanding interfacial redox reactions facilitated by transition metal oxides is critically important for the application of these materials in catalysis and energy storage. Over the past 20 years, a range of studies have described the relationship between the surface acid—base chemistry of transition metal oxides and their electronic properties. These contributions summarize the use of proton—electron codoping mechanisms as routes for tuning band edge energies, mediating phase transitions, and manipulating the surface structure of the material. With particular relevance to the surface dynamics of protons and transition metal oxides, convincing evidence has been provided that these materials participate in proton-coupled electron transfer (PCET). These results include thermodynamic descriptors of these redox processes that shape our thinking about limits of chemical reactivity and energy conversion in these systems.

Despite substantial progress that has been made in this space, an atomic-level understanding of proton-electron codoping interactions at the oxide-terminated surface of transition metal oxides remains elusive. Proton interactions with the surface of a transition metal oxide can range from weak hydrogen bonding contacts, to the formal reduction of M-O bonds to form hydroxide (M-OH) and aqua (M-OH₂) surface ligands. ^{3-6,10,13} The bulk structure of transition metal oxides renders distinguishing between these types of metal oxide linkages through surface analysis challenging; while some reports have presented atomic resolution of surface defects through the use of scanning tunneling microscopy (STM), this analytical technique is capable of manipulating the structure of reactive entities at the surface of the material. 6,14-18 Additionally, the static analysis of samples via STM, following a molecular transformation, renders in situ characterization of reaction intermediates nearly impossible.

Toward an atomistic understanding of the interfacial reactivity of transition metal oxides, researchers have turned to homogeneous metal oxide clusters as models for extended

solids. These well-defined assemblies have gained further traction as atomically precise representatives of bulk systems. This is a result of work that has revealed confined electronic communication within transition metal ions that compose bulk metal oxides. Polyoxometalates (POMs), in particular, have been touted as excellent structural models of metal oxides. These clusters are composed of multiple transition metal oxyanions linked together by bridging oxygen atoms. With relevance to understanding proton—electron codoping mechanisms in reducible metal oxides, POMs possess rich redox chemistry that is significantly altered in the presence of protons. Possess

Studies focused on interactions between POMs and protons typically involve acidification of an aqueous solution containing the polyoxoanion; results have predominantly shown cation exchange processes, yielding metal oxide assemblies with one or more bridging hydroxyl ligands. An exception to this is a class of heteropoly "brown" architectures. These sixelectron reduced polyoxotungstates are generated via controlled potential electrolysis under acidic conditions, resulting in the formation of three terminal WIV—OH2 species at a single face of the cluster. It is important to note that without cluster reduction, protons bind to the Keggin ion at the bridging oxide ligands. These initial reports have inspired several studies demonstrating the use of H-doping in POM scaffolds for hydrogen storage.

Over the past three years, our research team has been studying a class of organofunctionalized vanadium oxide clusters as model systems for reducible metal oxides. 25,26,43-45

Received: April 8, 2020 Published: May 20, 2020



Scheme 1. Reactivity of 1-V₆O₇²⁻ with [HNEt₃]BF₄

The physicochemical properties of polyoxovanadate-alkoxide (POV-alkoxide) clusters, such as their Robin and Day Class II delocalized electronic structure, redox-activity, solubility in organic solvents, and numerous spectroscopic handles (e.g., ¹H NMR, infrared, electronic absorption spectroscopies) make them excellent candidates for in situ analysis of the surface reactivity of transition metal oxides. 46-48 With relevance to understanding the mechanisms of metal oxide mediated reactions, we have reported the formation of oxygen-atom vacancies in these assemblies, ^{25,43,44} as well as their oxygen atom transfer reactivity with organic and small molecule substrates. 25,43-

Motivated by recent reports summarizing proton-electron codoping mechanisms for the activation of $VO_{2}^{3,4}$ as well as a myriad of other studies probing acid-induced surface activation of transition metal oxides, 5,9,49-52 we became interested in exploring the stoichiometric reactivity of POV-alkoxide clusters with organic acids. Dropwise addition of 1 equiv of triethylammonium tetrafluoroborate ([HNEt3]BF4) to a teal solution of the reduced, dianionic POV-alkoxide cluster, $[V_6O_7(OC_2H_5)_{12}]^{2-} \; (\text{1-V}_6O_7^{\; 2-}; \; e^- \; \text{distrib:} \; V^{IV}_{\;\; 6}), \; \text{resulted} \; \; \text{in}$ a striking color change from teal to brown-green over the course of 5 min (Scheme 1). Analysis of the crude reaction mixture by ¹H NMR spectroscopy revealed a series of paramagnetically shifted and broadened resonances, consistent with the formation of a mixture of products in an approximate 1:1 ratio (Figure 1; ratio of product formation determined by integration of signals corresponding to the distinct cluster species; see Figure S1 for details). Signals located at 26.07 and -2.00 ppm correspond to the protons of the bridging ethoxide

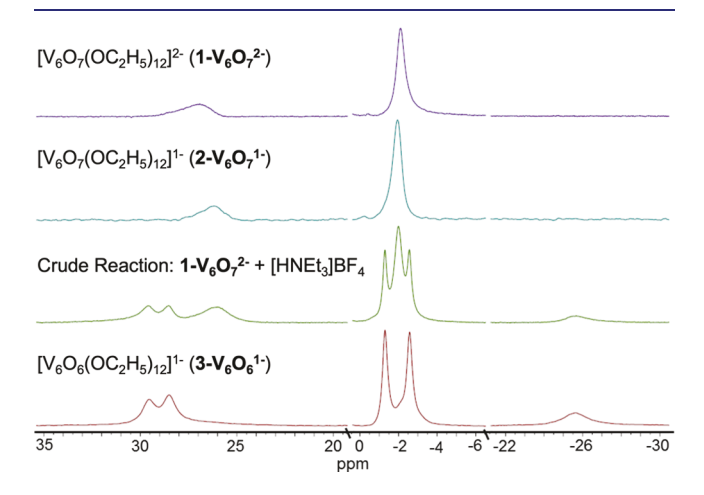


Figure 1. ¹H NMR analysis of acid addition reaction mixture (green), with independently synthesized clusters as references ($1-V_6O_7^{2-}$, purple; $2-V_6O_7^{1-}$, blue; $3-V_6O_6^{1-}$, red) in acetonitrile- d_3 .

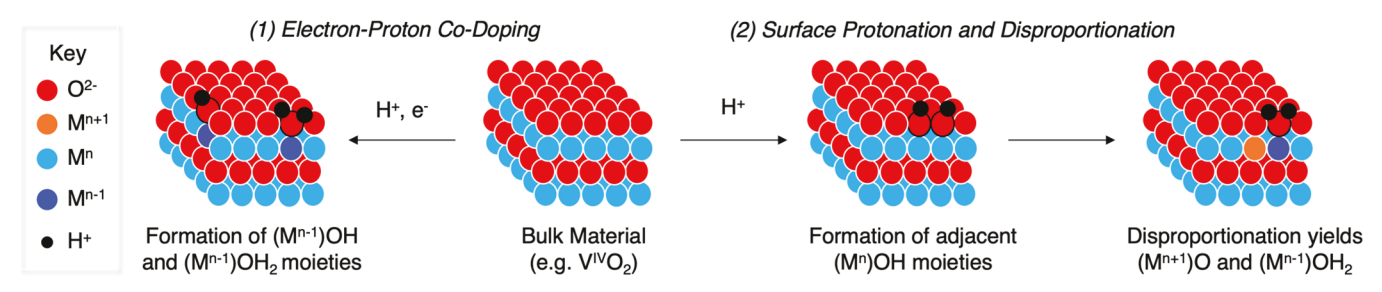
moieties of the monoanionic, POV-ethoxide cluster, $[V_6O_7(OC_2H_5)_{12}]^{1-}$ (2- $V_6O_7^{1-}$).⁵³ The remaining resonances, located at 29.56, 28.53, -1.30, -2.56, and -25.66 ppm, suggest formation of an organofunctionalized POV cluster with reduced symmetry as compared to the starting material. Previous results from our laboratory have shown similar patterns of signals corresponding to POV-ethoxide clusters bearing a single, site-differentiated vanadium center. 26,44 However, these POV-ethoxide clusters (e.g., $[V_6O_6(OC_2H_5)_{12}], [V_6O_6Cl(OC_2H_5)_{12}]^{1-})$ did not possess resonances that matched the unidentified product following acid addition to $1-V_6O_7^{2-}$.

To gain further insight into the molecular composition of the products of acid addition to $1-V_6O_7^{2-}$, electrospray ionization mass spectrometry (ESI-MS) was employed. Analysis of the resultant spectrum revealed three major signals (m/z = 958, 961, 974; ESI-MS(-)ve mode, Figure S2). The first signal, observed at m/z = 958, corresponds to complex 2- $V_6O_7^{1-}$, consistent with ¹H NMR analysis of the crude sample. The remaining signals could be assigned to an oxygen-deficient POV-alkoxide cluster, $[V_6O_6(OC_2H_5)_{12}]^{1-} (3-V_6O_6^{1-})$, plus either a hydronium ion (m/z = 961), or an equivalent of methanol (m/z = 974).

To confirm formation of complex $3-V_6O_6^{1-}$, independent synthesis of the cluster was performed via reduction of the previously reported oxygen-deficient POV-ethoxide cluster, $[V_6O_6(OC_2H_5)_{12}]^0$ (see Supporting Information for details).⁴ Characterization of the crude product by ESI-MS showed a main signal at m/z = 974 (Figure S3). Following workup, analysis of the product by ¹H NMR spectroscopy revealed a set of five paramagnetically shifted resonances, distinct from that of the starting material ($\delta = 29.59, 28.54, -1.28, -2.56, \text{ and}$ -25.60 ppm; Figure 2). These data match those corresponding to the unidentified product of acid addition to $1-V_6O_7^{2-}$ (vide

The electronic structure of the oxygen-deficient POVethoxide cluster was examined by infrared and electronic absorption spectroscopies (Figures S4-S5, Table S1). In the IR spectra, two broad absorption bands centered at 1049 and 951 cm⁻¹ were observed and correspond to $\nu(O_b-C_2H_5)$ (O_b = bridging oxide) and $\nu(V=O_t)$ (O_t = terminal oxo), respectively. These features resemble those reported for the anionic, methoxide-bridged analogue $([V_6O_6(OCH_3)_{12}]^{1-}$: 1047 cm⁻¹, 951 cm⁻¹), consistent with formation of the reduced ethoxide-bridged species.²⁵ The electronic absorption spectrum presents further evidence for reduction of the hexavanadate core in $3\text{-}V_6O_6^{1-}$. The starting material, $[V_6O_6(OC_2H_5)_{12}]^0$, contains two intervalence charge transfer (IVCT) bands at 394 nm ($\varepsilon = 2793 \text{ M}^{-1} \text{ cm}^{-1}$) and 1000 nm $(\varepsilon = 417 \text{ M}^{-1} \text{ cm}^{-1})$ associated with an electron transfer from $V^{IV} \rightarrow V^{V}$ ions within the cluster core.⁴⁴ The lack of these

Mechanisms of Acid-induced "M-OH2" Formation at Reducible Metal Oxide Surfaces



This Work: Acid-induced O-atom Vacancy Formation in POV-alkoxide Clusters

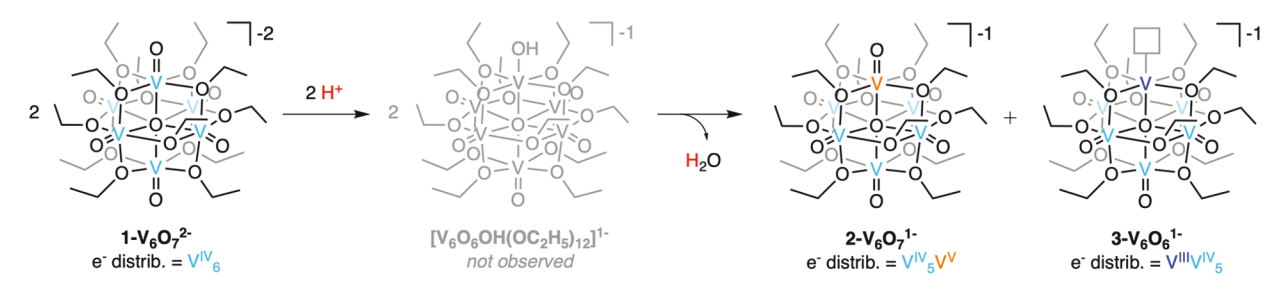


Figure 2. Schematic representation of proton-induced activation on a metal oxide surface (top), and the comparable reactivity observed on a POV-alkoxide cluster (bottom).

IVCT bands observed in the absorption spectra of $3\text{-V}_6\mathbf{O}_6^{\ 1^-}$ is consistent with the reduction of the V^V ion in the neutral monovacant cluster to a V^{IV} center. Furthermore, the weak transition observed at 536 nm ($\varepsilon=502\ \text{M}^{-1}\ \text{cm}^{-1}$) matches that of previously reported oxygen-deficient polyanions in their most-reduced charge state. Collectively, these characterization techniques suggest an oxidation state distribution of vanadium ions for $3\text{-V}_6\mathbf{O}_6^{\ 1^-}$ of $(V^{III}V^{IV}_5)$, matching that reported for the monoanionic POV-methoxide cluster with a single oxygen atom vacancy, $[V_6O_6(O\text{CH}_3)_{12}]^{1-25}$

The electronic structure of complex $3 \cdot V_6 O_6^{-1-}$ is notable in light of recent studies summarizing the reactivity of VO2 films with acid (Figure 2, Mechanism 1).^{3,4} Upon exposure to acidic media in the presence of an external reductant, formation of an electron-proton codoped material is observed.^{3,4} X-ray photoelectron spectroscopy (XPS) and X-ray absorption near-edge structure (XANES) measurements on the resultant films indicated that VIV ions of the material were partially reduced to VIII centers. Additionally, spectroscopic analysis revealed features corresponding to the reduction in bond order of V=O linkages to hydroxide moieties. Similarly, the addition of acid to complex $1-V_6O_7^{2-}$ results in formation of a surface VIII ion and reduction of a vanadyl moiety. However, whereas, in the case of the bulk material, the site-specific structure of reduced vanadium centers is proposed to be VIII-OH moieties, characterization of our molecular species suggests the formation of a V^{III}-OH₂ adduct (note: in the case of our POV-ethoxide cluster, the datively bound, surface water ligand is displaced by acetonitrile). The presence of this "vacant" metal cation embedded within the vanadium oxide cluster via acid-induced reduction offers an alternative explanation for the surface site composition following acid-base chemistry on extended solids.

The resultant reduced, oxygen-deficient POV-alkoxide cluster, $3\text{-V}_6\mathrm{O}_6^{1-}$, formed by addition of acid necessitates consideration of the source of reducing equivalents for this oxidation state distribution of vanadium centers ($\mathrm{V^{III}V^{IV}}_5$, vide

supra). In the interest of providing a tentative explanation for the formation of $3-V_6O_6^{1-}$ in the absence of an external reductant, we pose that protonation of a terminal vanadyl would result in transient formation of a VIV-OH moiety. This hypothesis is supported by a previously reported acid dissociation constant for a molecular vanadium(IV) hydroxyl complex, $[(^{tBu2}bipy)_2VO(OH)]^+$ (p $K_a = 36.7$), that would suggest that proton transfer from [HNEt₃]⁺ to a V^{IV}=O moiety of the cluster would be thermodynamically favorable.⁵ Subsequently, the unstable, hydroxide-functionalized POVethoxide cluster can undergo rapid disproportionation, resulting in the formation of $2-V_6O_7^{1-}$, $3-V_6O_6^{1-}$, and H_2O (i.e., $V^{IV} \rightarrow V^{V} + V^{III}$; Figure 2). Indeed, theoretical investigations into the reactivity of vanadium oxides with acid support that the formation of surface V-OH2 moieties is preferred, given that the subsequent desorption of the H₂O results in the formation of an oxygen-deficient site, which can be stabilized via vacancy-induced lattice relaxation (Figure 2, Mechanism 2). 55 Likewise, similar mechanisms of acid-induced vacancy formation have been reported for other reducible metal oxides (e.g., TiO₂, ZnO).^{6,8} It is important to note that, at this juncture, this mechanism is speculative and the subject of ongoing investigations in our laboratory.

Here, we present a new route for the formation of an oxygen-deficient Lindqvist cluster via addition of a weak organic acid to the dianionic POV-ethoxide, $1\text{-}V_6\text{O}_7^{2\text{-}}$. This activity is previously unobserved, being differentiated from other heteropoly "brown" complexes in that the cluster itself contains the electron density required for proton-directed M=O bond activation, where typically this must be added electrochemically during or after cluster synthesis. $^{36-39}$ Overall, our results present an atomic-level model for understanding the physicochemical consequences of acid treatment of redox-active transition metal oxides. The study of atomically precise POV-alkoxides that are soluble in organic solvents enables us to fill fundamental gaps in materials science research, specifically the nature of proton-induced surface

activation via electron—proton codoping mechanisms. Where a multitude of reports have given insight into the physicochemical consequences of codoping bulk transition metal oxides, acquiring sufficient details about the precise activity at a single lattice site remains challenging. By using polynuclear assemblies as a model system for heterogeneous catalysts, we can access the necessary precision to analyze proton interactions with POV-alkoxide clusters.

ASSOCIATED CONTENT

5 Supporting Information

The Supporting Information is available free of charge at https://pubs.acs.org/doi/10.1021/jacs.0c03864.

Materials, experimental procedures, and characterization for all compounds; ^{1}H NMR and ESI-MS(–)ve spectra of acid addition to $1\text{-V}_{6}O_{7}^{2-}$, ^{1}H NMR, ESI-MS(–)ve, IR, and electronic absorption spectra of $3\text{-V}_{6}O_{6}^{1-}$ and cyclic voltammogram of $1\text{-V}_{6}O_{7}^{2-}$ (PDF)

AUTHOR INFORMATION

Corresponding Author

Ellen M. Matson — Department of Chemistry, University of Rochester, Rochester, New York 14627, United States; orcid.org/0000-0003-3753-8288; Email: matson@chem.rochester.edu

Authors

Eric Schreiber — Department of Chemistry, University of Rochester, Rochester, New York 14627, United States Brittney E. Petel — Department of Chemistry, University of Rochester, Rochester, New York 14627, United States

Complete contact information is available at: https://pubs.acs.org/10.1021/jacs.0c03864

Notes

The authors declare no competing financial interest.

■ ACKNOWLEDGMENTS

This research was funded by the National Science Foundation through Grant CHE-1653195. E.M.M. is a recipient of a Cottrell Award from the Research Corporation for Science Advancement, which has provided additional resources to support this research. The authors thank Alex A. Fertig for helpful discussions and assistance in the synthesis of starting materials. The authors also acknowledge generous financial support from the University of Rochester through start-up funds.

REFERENCES

- (1) Manjakkal, L.; Szwagierczak, D.; Dahiya, R. Metal Oxides Based Electrochemical PH Sensors: Current Progress and Future Perspectives. *Prog. Mater. Sci.* **2020**, *109*, 100635.
- (2) Valdez, C. N.; Braten, M.; Soria, A.; Gamelin, D. R.; Mayer, J. M. Effect of Protons on the Redox Chemistry of Colloidal Zinc Oxide Nanocrystals. *J. Am. Chem. Soc.* **2013**, *135*, 8492–8495.
- (3) Chen, Y.; Wang, Z.; Chen, S.; Ren, H.; Wang, L.; Zhang, G.; Lu, Y.; Jiang, J.; Zou, C.; Luo, Y. Non-Catalytic Hydrogenation of VO 2 in Acid Solution. *Nat. Commun.* **2018**, *9*, 1–8.
- (4) Li, B.; Xie, L.; Wang, Z.; Chen, S.; Ren, H.; Chen, Y.; Wang, C.; Zhang, G.; Jiang, J.; Zou, C. Electron-Proton Co-Doping-Induced Metal-Insulator Transition in VO2 Film via Surface Self-Assembled l-Ascorbic Acid Molecules. *Angew. Chem., Int. Ed.* **2019**, *58*, 13711–13716.

- (5) Lyon, L. A.; Hupp, J. T. Energetics of the Nanocrystalline Titanium Dioxide/Aqueous Solution Interface: Approximate Conduction Band Edge Variations between H0 = -10 and H- = +26. *J. Phys. Chem. B* **1999**, *103*, 4623–4628.
- (6) Aizawa, M.; Morikawa, Y.; Namai, Y.; Morikawa, H.; Iwasawa, Y. Oxygen Vacancy Promoting Catalytic Dehydration of Formic Acid on TiO₂(110) by in Situ Scanning Tunneling Microscopic Observation. *J. Phys. Chem. B* **2005**, *109*, 18831–18838.
- (7) Li, Z.; Shen, W.; Zhang, X.; Fang, L.; Zu, X. Controllable Growth of SnO₂ Nanoparticles by Citric Acid Assisted Hydrothermal Process. *Colloids Surf., A* **2008**, 327, 17–20.
- (8) Liu, T.; Li, Y.; Zhang, H.; Wang, M.; Fei, X.; Duo, S.; Chen, Y.; Pan, J.; Wang, W. Tartaric Acid Assisted Hydrothermal Synthesis of Different Flower-like ZnO Hierarchical Architectures with Tunable Optical and Oxygen Vacancy-Induced Photocatalytic Properties. *Appl. Surf. Sci.* **2015**, 357, 516–529.
- (9) Yang, X.; Yu, X.; Lin, M.; Ma, X.; Ge, M. Enhancement Effect of Acid Treatment on Mn₂O₃ Catalyst for Toluene Oxidation. *Catal. Today* **2019**, 327, 254–261.
- (10) Schrauben, J. N.; Hayoun, R.; Valdez, C. N.; Braten, M.; Fridley, L.; Mayer, J. M. Titanium and Zinc Oxide Nanoparticles Are Proton-Coupled Electron Transfer Agents. *Science* **2012**, *336*, 1298–1301.
- (11) Braten, M. N.; Gamelin, D. R.; Mayer, J. M. Reaction Dynamics of Proton-Coupled Electron Transfer from Reduced ZnO Nanocrystals. *ACS Nano* **2015**, *9*, 10258–10267.
- (12) Ghosh, S.; Castillo-Lora, J.; Soudackov, A. V.; Mayer, J. M.; Hammes-Schiffer, S. Theoretical Insights into Proton-Coupled Electron Transfer from a Photoreduced ZnO Nanocrystal to an Organic Radical. *Nano Lett.* **2017**, *17*, 5762–5767.
- (13) Wise, C. F.; Mayer, J. M. Electrochemically Determined O-H Bond Dissociation Free Energies of NiO Electrodes Predict Proton-Coupled Electron Transfer Reactivity. *J. Am. Chem. Soc.* **2019**, *141*, 14971–14975.
- (14) Pang, C. L.; Lindsay, R.; Thornton, G. Chemical Reactions on Rutile TiO₂(110). *Chem. Soc. Rev.* **2008**, *37*, 2328–2353.
- (15) Pacchioni, G.; Freund, H. Electron Transfer at Oxide Surfaces. The MgO Paradigm: From Defects to Ultrathin Films. *Chem. Rev.* **2013**, *113*, 4035–4072.
- (16) Ruiz Puigdollers, A.; Schlexer, P.; Tosoni, S.; Pacchioni, G. Increasing Oxide Reducibility: The Role of Metal/Oxide Interfaces in the Formation of Oxygen Vacancies. *ACS Catal.* **2017**, *7*, 6493–6513.
- (17) Glass, D.; Cortés, E.; Ben-Jaber, S.; Brick, T.; Peveler, W. J.; Blackman, C. S.; Howle, C. R.; Quesada-Cabrera, R.; Parkin, I. P.; Maier, S. A. Dynamics of Photo-Induced Surface Oxygen Vacancies in Metal-Oxide Semiconductors Studied Under Ambient Conditions. *Adv. Sci.* 2019, *6*, 1901841.
- (18) Iwasawa, Y.; Onishi, H.; Fukui, K.; Suzuki, S.; Sasaki, T. The Selective Adsorption and Kinetic Behaviour of Molecules on $TiO_2(110)$ Observed by STM and NC-AFM. Faraday Discuss. 1999, 114, 259–266.
- (19) Biswas, S.; Husek, J.; Londo, S.; Baker, L. R. Highly Localized Charge Transfer Excitons in Metal Oxide Semiconductors. *Nano Lett.* **2018**, *18*, 1228–1233.
- (20) Biswas, S.; Husek, J.; Baker, L. R. Elucidating Ultrafast Electron Dynamics at Surfaces Using Extreme Ultraviolet (XUV) Reflection-Absorption Spectroscopy. *Chem. Commun.* **2018**, *54*, 4216–4230.
- (21) Biswas, S.; Husek, J.; Londo, S.; Fugate, E. A.; Baker, L. R. Identifying the Acceptor State in NiO Hole Collection Layers: Direct Observation of Exciton Dissociation and Interfacial Hole Transfer across a Fe₂O₃/NiO Heterojunction. *Phys. Chem. Chem. Phys.* **2018**, 20, 24545–24552.
- (22) Day, V. W.; Fredrich, M. F.; Klemperer, W. G.; Liu, R. S. Polyoxomolybdate-Hydrocarbon Interactions. Synthesis and Structure of the $\mathrm{CH_2Mo_4O_{15}H_3}^-$ Anion and Related Methylenedioxymolybdates. *J. Am. Chem. Soc.* **1979**, *101*, 491–492.
- (23) Gómez-Romero, P. Polyoxometalates as Photoelectrochemical Models for Quantum-Sized Colloidal Semiconducting Oxides. *Solid State Ionics* **1997**, *101*–*103*, 243–248.

- (24) Kholdeeva, O. A.; Maksimovskaya, R. I. Titanium- and Zirconium-Monosubstituted Polyoxometalates as Molecular Models for Studying Mechanisms of Oxidation Catalysis. *J. Mol. Catal. A: Chem.* **2007**, 262, 7–24.
- (25) Petel, B. E.; Brennessel, W. W.; Matson, E. M. Oxygen-Atom Vacancy Formation at Polyoxovanadate Clusters: Homogeneous Models for Reducible Metal Oxides. *J. Am. Chem. Soc.* **2018**, *140*, 8424–8428.
- (26) Petel, B. E.; Meyer, R. L.; Maiola, M. L.; Brennessel, W. W.; Müller, A. M.; Matson, E. M. Site-Selective Halogenation of Polyoxovanadate Clusters: Atomically Precise Models for Electronic Effects of Anion Doping in VO₂. J. Am. Chem. Soc. **2020**, 142, 1049–1056
- (27) Song, Y.-F.; Tsunashima, R. Recent Advances on Polyoxometalate-Based Molecular and Composite Materials. *Chem. Soc. Rev.* **2012**, *41*, 7384–7402.
- (28) Sadayuki, H.; Hideki, T.; Masato, H. Synthesis, Structure, and Characterization of an α -Dawson-Type $[S_2W_{18}O_{62}]^{4-}$ Complex. Bull. Chem. Soc. Ipn. **2001**, 74, 1623–1628.
- (29) Zhou, C.; Li, S.; Zhu, W.; Pang, H.; Ma, H. A Sensor of a Polyoxometalate and Au-Pd Alloy for Simultaneously Detection of Dopamine and Ascorbic Acid. *Electrochim. Acta* **2013**, *113*, 454–463.
- (30) Sun, W.; He, C.; Liu, T.; Duan, C. Synergistic Catalysis for Light-Driven Proton Reduction Using a Polyoxometalate-Based Cu-Ni Heterometallic-Organic Framework. *Chem. Commun.* **2019**, 55, 3805–3808.
- (31) Tucher, J.; Nye, L. C.; Ivanovic-Burmazovic, I.; Notarnicola, A.; Streb, C. Chemical and Photochemical Functionality of the First Molecular Bismuth Vanadium Oxide. *Chem. Eur. J.* **2012**, *18*, 10949–10953.
- (32) Chen, Q.; Goshorn, D. P.; Scholes, C. P.; Tan, X. L.; Zubieta, J. Coordination Compounds of Polyoxovanadates with a Hexametalate Core. Chemical and Structural Characterization of $[V^V_{6}O_{13}[(OCH_2)_3CR]_2]^2$, $[V^V_{6}O_{11}(OH)_2[(OCH_2)_3CR]_2]$, $[V^{IV}_{4}V^V_{2}O_9(OH)_4[(OCH_2)_3CR]_2]^2$, and $[V^{IV}_{6}O_7(OH)_6]$ - $(OCH_2)_3CR]_2]^2$. J. Am. Chem. Soc. 1992, 114, 4667–4681.
- (33) Arana, G.; Etxebarria, N.; Fernandez, L. A.; Madariaga, J. M. Hydrolysis of Nb(V) and Ta(V) in Aqueous KCl at 25°C. Part II: Construction of a Thermodynamic Model for Ta(V). *J. Solution Chem.* 1995, 24, 611–622.
- (34) Etxebarria, N.; Fernández, L. A.; Madariaga, J. M. On the Hydrolysis of Niobium(V) and Tantalum(V) in 3 Mol Dm⁻³ KCl at 25 °C. Part 1. Construction of a Thermodynamic Model for NbV. *J. Chem. Soc., Dalton Trans.* 1994, 3055–3059.
- (35) Day, V. W.; Klemperer, W. G.; Maltbie, D. J. Where Are the Protons in $H_3V_{10}O_{28}^{3-2}$? J. Am. Chem. Soc. 1987, 109, 2991–3002.
- (36) Launay, J. P. Reduction of the metatungstate ion. High levels of reduction of $H_2W_{12}O_{40}{}^6$, derivatives of the ion $HW_{12}O_{40}{}^7$ and general discussion. *J. Inorg. Nucl. Chem.* **1976**, 38, 807–816.
- (37) Kazansky, L. P.; Launay, J. P. X-Ray Photoelectron Study of Mixed Valence Metatungstate Anions. *Chem. Phys. Lett.* **1977**, *51*, 242–245.
- (38) Jeannin, Y.; Launay, J. P.; Sedjadi, M. A. S. Crystal and Molecular Structure of the Six-Electron-Reduced Form of Metatung-state $Rb_4H_8[H_2W_{12}O_{40}]$. Apprx.18 H_2O : Occurrence of a Metal-Metal Bonded Subcluster in a Heteropolyanion Framework. *Inorg. Chem.* **1980**, *19*, 2933–2935.
- (39) Piepgrass, K.; Pope, M. T. Heteropoly "Brown" as Class I Mixed Valence (W(IV, VI)) Complexes. Tungsten-183 NMR of W(IV) Trimers. J. Am. Chem. Soc. 1987, 109, 1586–1587.
- (40) Yang, J.; Janik, M. J.; Ma, D.; Zheng, A.; Zhang, M.; Neurock, M.; Davis, R. J.; Ye, C.; Deng, F. Location, Acid Strength, and Mobility of the Acidic Protons in Keggin 12-H₃PW₁₂O₄₀: A Combined Solid-State NMR Spectroscopy and DFT Quantum Chemical Calculation Study. *J. Am. Chem. Soc.* **2005**, *127*, 18274–18280.
- (41) Itagaki, S.; Yamaguchi, K.; Mizuno, N. Heteropoly Acid-Based Materials for Reversible H₂ Storage as Protons and Electrons under Mild Conditions. *Chem. Mater.* **2011**, 23, 4102–4104.

- (42) Aspera, S. M.; Arevalo, R. L.; Nakanishi, H.; Kasai, H.; Sekine, S.; Kawai, H. Vanadium Doped Polyoxometalate: Induced Active Sites and Increased Hydrogen Adsorption. *J. Phys.: Condens. Matter* **2020**, 32, 195001.
- (43) Petel, B. E.; Fertig, A. A.; Maiola, M. L.; Brennessel, W. W.; Matson, E. M. Controlling Metal-to-Oxygen Ratios via M-O Bond Cleavage in Polyoxovanadate Alkoxide Clusters. *Inorg. Chem.* **2019**, 58, 10462–10471.
- (44) Petel, B. E.; Meyer, R. L.; Brennessel, W. W.; Matson, E. M. Oxygen Atom Transfer with Organofunctionalized Polyoxovanadium Clusters: O-Atom Vacancy Formation with Tertiary Phosphanes and Deoxygenation of Styrene Oxide. *Chem. Sci.* **2019**, *10*, 8035–8045.
- (45) Petel, B. E.; Matson, E. M. Conversion of NO_x^{1-} (x = 2, 3) to NO Using an Oxygen-Deficient Polyoxovanadate-Alkoxide Cluster. *Chem. Commun.* **2020**, *56*, 555–558.
- (46) Robin, M. B.; Day, P. Mixed Valence Chemistry-A Survey and Classification. In *Adv. Inorg. Chem. Radiochem.*; Emeléus, H. J., Sharpe, A. G., Eds.; Academic Press, 1968; Vol. 10, pp 247–422.
- (47) Spandl, J.; Daniel, C.; Brüdgam, I.; Hartl, H. Synthesis and Structural Characterization of Redox-Active Dodecamethoxoheptaoxohexavanadium Clusters. *Angew. Chem., Int. Ed.* **2003**, *42*, 1163–1166
- (48) Daniel, C.; Hartl, H. Neutral and Cationic V^{IV}/V^V Mixed-Valence Alkoxo-Polyoxovanadium Clusters $[V6O7(OR)_{12}]^{n+}$ (R = -CH₃, -C₂H₅): Structural, Cyclovoltammetric and IR-Spectroscopic Investigations on Mixed Valency in a Hexanuclear Core. *J. Am. Chem. Soc.* 2005, 127, 13978–13987.
- (49) Ai, M. Activities for the Decomposition of Formic Acid and the Acid-Base Properties of Metal Oxide Catalysts. *J. Catal.* **1977**, *50*, 291–300.
- (50) Busca, G. Spectroscopic Characterization of the Acid Properties of Metal Oxide Catalysts. *Catal. Today* **1998**, *41*, 191–206.
- (51) Nüesch, F.; Kamarás, K.; Zuppiroli, L. Protonated Metal-Oxide Electrodes for Organic Light Emitting Diodes. *Chem. Phys. Lett.* **1998**, 283, 194–200.
- (52) Quiroz, J.; Giraudon, J.-M.; Gervasini, A.; Dujardin, C.; Lancelot, C.; Trentesaux, M.; Lamonier, J.-F. Total Oxidation of Formaldehyde over MnO_x - CeO_2 Catalysts: The Effect of Acid Treatment. *ACS Catal.* **2015**, *5*, 2260–2269.
- (53) VanGelder, L. E.; Kosswattaarachchi, A. M.; Forrestel, P. L.; Cook, T. R.; Matson, E. M. Polyoxovanadate-Alkoxide Clusters as Multi-Electron Charge Carriers for Symmetric Non-Aqueous Redox Flow Batteries. *Chem. Sci.* **2018**, *9*, 1692–1699.
- (54) McCarthy, B. D.; Martin, D. J.; Rountree, E. S.; Ullman, A. C.; Dempsey, J. L. Electrochemical Reduction of Brønsted Acids by Glassy Carbon in Acetonitrile—Implications for Electrocatalytic Hydrogen Evolution. *Inorg. Chem.* **2014**, *53*, 8350–8361.
- (55) Hermann, K.; Witko, M.; Druzinic, R. Electronic Properties, Structure and Adsorption at Vanadium Oxide: Density Functional Theory Studies. *Faraday Discuss.* **1999**, *114*, 53–66.